Signaling transduction regulated by 5-hydroxytryptamine 1A receptor and

orexin receptor 2 heterodimers

Qin-Qin Wang[a], Chun-Mei Wang[a], Bao-Hua Cheng[a], Chun-Qing Yang[a], Bo Bai[a]*, Jing Chen[a,b]*

[a]Neurobiology Key Laboratory of Jining Medical University in Colleges of Shandong, Jining, 272067, P.R. of China; wq19870917@163.com (Q.-Q.W.); wangchunmei410@163.com (C.-M.W.); chengbh1979@163.com (B.-H.C.); ycqangel@126.com (C.-Q.Y.)

[b]Division of Biomedical Sciences, Warwick Medical School, University of Warwick, Coventry, CV4 7AL, UK.

*Corresponding authors: Division of Biomedical Sciences, Warwick Medical School, University of Warwick, Coventry, Tel: +44 2476968693

E-mail addresses: bobai@mail.jnmc.edu.cn; Jing.Chen@warwick.ac.uk.

Abstract

As G-protein-coupled receptors (GPCRs), 5-hydroxytryptamine 1A receptor (5-HT1AR) and orexin receptor 2 (OX2R) regulate the levels of the cellular downstream molecules. The heterodimers of different GPCRs play important roles in various of neurological diseases. Moreover, 5-HT1AR and OX2R are involved in the pathogenesis of neurological diseases such as depression with deficiency of hippocampus plasticity. However, the direct interaction of the two receptors remains elusive. In the present study, we firstly demonstrated the heterodimer formation of 5-HT1AR and OX2R. Exchange protein directly activated by cAMP (Epac) cAMP bioluminescence resonance energy transfer (BRET) biosensor analysis revealed that the expression levels of cellular cAMP significantly increased in HEK293T cells transfected with the two receptors compared with the 5-HT1AR group. Additionally, the cellular level of calcium was upregulated robustly in HEK293T cells co-transfected with 5-HT1AR and OX2R group after agonist treatment. Furthermore, western blotting data showed that 5-HT1AR and OX2R heterodimer decreased the levels of phosphorylation of extracellular signal-regulated kinase (ERK) and cAMP-response element-binding protein (CREB). These results not only unraveled the formation of 5-HT1AR and OX2R heterodimer but also suggested that the heterodimer affected the downstream signaling pathway, which will provide new insights into the function of the two receptors in the brain.

Introduction

G-protein-coupled receptors (GPCRs) are critical in regulating a variety of physiological processes including cell growth, cell survival, cell migration and metabolism [1-3]. Previous research showed that deficiency in the function of GPCRs resulted in the progresses of the pathology of brain disorders [4, 5], suggesting the important role of GPCRs in the brain and the possibility of GPCRs as therapeutic targets for neurological diseases. More importantly, evidence has revealed that different GPCRs formed heterodimer and were involved in different physiological and pathological processes. The heteroreceptor of Dopamine D2 receptor (Drd2) and Disrupted in Schizophrenia 1 (DISC1) increased the glycogen synthase kinase (GSK)-3 signaling regulated by Drd2, which leading to the antipsychotic-like effects [6]. Moreover, the heteroreceptor of galanin receptor 1 (GalR1) and 5-HT1AR has been proposed to be involved in the antidepressant effects caused by zinc [7, 8]. These observations provide new insights into the cellular mechanism during the pathogenesis of neurological diseases [9, 10].

5-hydroxytryptamine receptors play important roles in cellular signaling regulation. There are seven subtypes of 5-hydroxytryptamine receptors including 5-hydroxytryptamine 1A receptor (5-HT1AR), 5-hydroxytryptamine 2 receptor (5-HT2R), 5-hydroxytryptamine 3 receptor (5-HT3R), 5-hydroxytryptamine 4 receptor (5-HT4R), 5-hydroxytryptamine 5 receptor (5-HT5R), 5-hydroxytryptamine 6 receptor (5-HT6R) and 5-hydroxytryptamine 7 receptor (5-HT7R) [11, 12]. As one member of these receptors, 5-HT1AR has been reported to express widely in the brain areas including hippocampus, hypothalamus and midbrain. Additionally, increasing amounts of evidence indicated that 5-HT1AR is critical for lots of physiological function such as cognition and emotion control [13, 14]. 5-HT1AR mainly binds to the Gi protein resulting in the reduction of adenylate cyclase (AC) activation, and further leads to the downregulation of the expression levels of p-CREB and cellular

cAMP calcium levels after ligand stimulation [15]. Moreover, 5-HT1AR has been proposed to form heterodimers with other GPCRs and is involved in the regulation of cellular signaling pathway. Previous studies have suggested that 5-HT1AR homodimer activation reduced the level of cellular cAMP, while the heterodimers of 5-HT1AR and dopaminergic receptor 2 (Drd2) led to potentiation of cAMP levels following the agonist 8-OHDPAT treatment [10]. Additionally, co-activation of 5-HT1AR and fibroblast growth factor receptor 1 (FGFR1) heterodimer by 8-OHDPAT and FGF2 induced the upregulation of phosphorylated extracellular signal-regulated kinase (p-ERK) and increased the neurite densities of primary hippocampal neurons [16]. These results demonstrated the important role of 5-HT1AR in GPCRs heterodimer functions.

Analogously, orexin receptor 2 (OX2R) expresses extensively in adult brain including cerebral cortex, hippocampus and cerebellum [17]. As a member of GPCRs, OX2R binds to the Gs protein and Gq protein resulting in the activation of adenylate cyclase (AC), and further leads to the upregulation of the expression levels of p-CREB, p-ERK, cellular cAMP and calcium levels after ligand orexin A or orexin B stimulation [18-20]. More interestingly, the expression of OX2R gradually decreased with age [17], indicating the potential role of OX2R in aging. Current research showed that orexin/OX2R signaling mainly regulated the processes of sleep, reward, feeding, pain and endocrine [21-24]. Behavior experiments demonstrated that mice with OX2R deficiency displayed an increase of despair, suggesting the important role of OX2R in brain disorders [25].

Although 5-HT1AR and OX2R are belonged to the GPCRs family, activate the downstream signaling pathway to regulate various of physiological processes [13, 14, 17], whether these two receptors could form heterodimers has been less studied.

In the present study, we firstly found 5-HT1AR and OX2R form heterodimer in HEK293T cells and in hippocampus. Furthermore, co-activation of 5-HT1AR-OX2R heterodimer led to a significant increase of cellular cAMP and calcium influx compared with the 5-HT1AR transfected group in HEK293T cells. In contrast, compared with the 5-HT1AR or OX2R transfected group, the expression levels of

p-ERK and p-CREB were decreased robustly following the agonists stimulation in 5-HT1AR and OX2R co-transfected group. Our findings provide new insights into role of 5-HT1AR and OX2R in the brain function.

RESULTS

The heterodimer of 5-HT1AR and OX2R in hippocampus

To explore the existence of 5-HT1AR-OX2R heterodimers, we initially carried out Proximity Ligation Assay (PLA) on slices of rat hippocampus. Goat anti-5-HT1AR and rabbit anti-OX2R antibodies were used to perform PLA assay. After incubation of 5-HT1AR and OX2R antibodies, we detected stable fluorescence signal in the hippocampus slices (Figure 1A-C). In contrast, the control group was performed with only 5-HT1AR primary antibody followed by the incubation of both secondary antibodies and no signal was found in the control group (Figure 1D-F). DAPI was used to stain the nuclei (Figure 1B and Figure 1E). And the merged images of PLA signal and DAPI showed that 5-HT1AR and OX2R formed the heterodimers (Figure 1C and Figure 1F). The statistic results also demonstrated that 5-HT1AR and OX2R formed heterodimers in hippocampus (Figure 1G). This is the first evidence suggesting that the formation of 5-HT1AR-OX2R heterodimers in hippocampus.
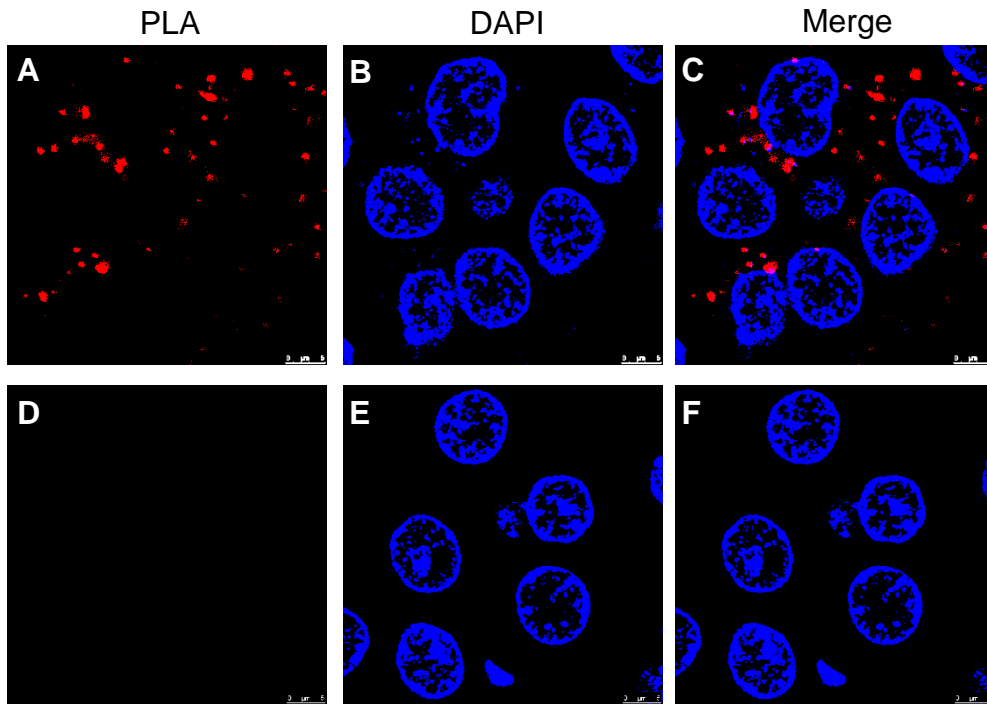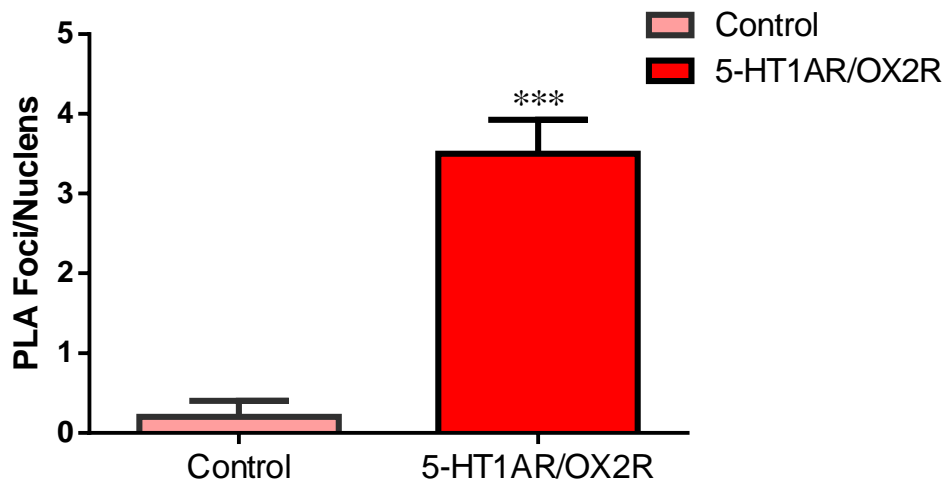
Figure 1. Direct interaction between 5-HT1AR and OX2R in the hippocampus of the adult rat.

(A-C) Representative photomicrographs staining with antibodies against 5-HT1AR and OX2R by PLA. Red dots represent the interaction of 5-HT1AR and OX2R (A). The nuclei were stained with DAPI (blue) (B). The merged photomicrograph in (C). Scale bars=5 μm.

ttsfadsdxf9aa">61</key></foreignraphs of control group incubating with 5-HT1AR primary antibody followed by the incubation with both the secondary antibodies by PLA (D). The nuclei were stained with DAPI (blue) (E). The merged photomicrograph in (F). Scale bars=5 μm.

(G) Statistics for PLA dots in (A-F).

5-HT1AR was co-localized with OX2R in the membrane of HEK293T cells

We next verified the co-localization of 5-HT1AR and OX2R. We used cell model to examine the expression pattern of 5-HT1AR and OX2R. 5-HT1AR-ECFP and OX2R-Venus plasmids were co-transfected into the HEK293T cell. The cells were transferred into the slides in the 12-well plate 24 h after the plasmids transfection. Sequentially, the fluorescence signals were analyzed using confocal microscopy 24 h following the cell passage. The results showed that the fluorescence signals of ECFP and Venus were significantly merged in the HEK293T cell membrane (Figure 2A-C). To exclude the possibility of ECFP affecting the localization of 5-HT1AR, we then transfected HEK293T cells using 5-HT1AR plasmid without any tags. Instead, immunostaining of 5-HT1AR by its antibody was performed to indicate the expression of 5-HT1AR after 48 h following the transfection. As shown in Figure 2, the fluorescence signals of 5-HT1AR antibody and Venus were also largely merged in HEK293T cells (Figure 2D-F). These results provide the evidence that 5-HT1AR is co-localized with OX2R.
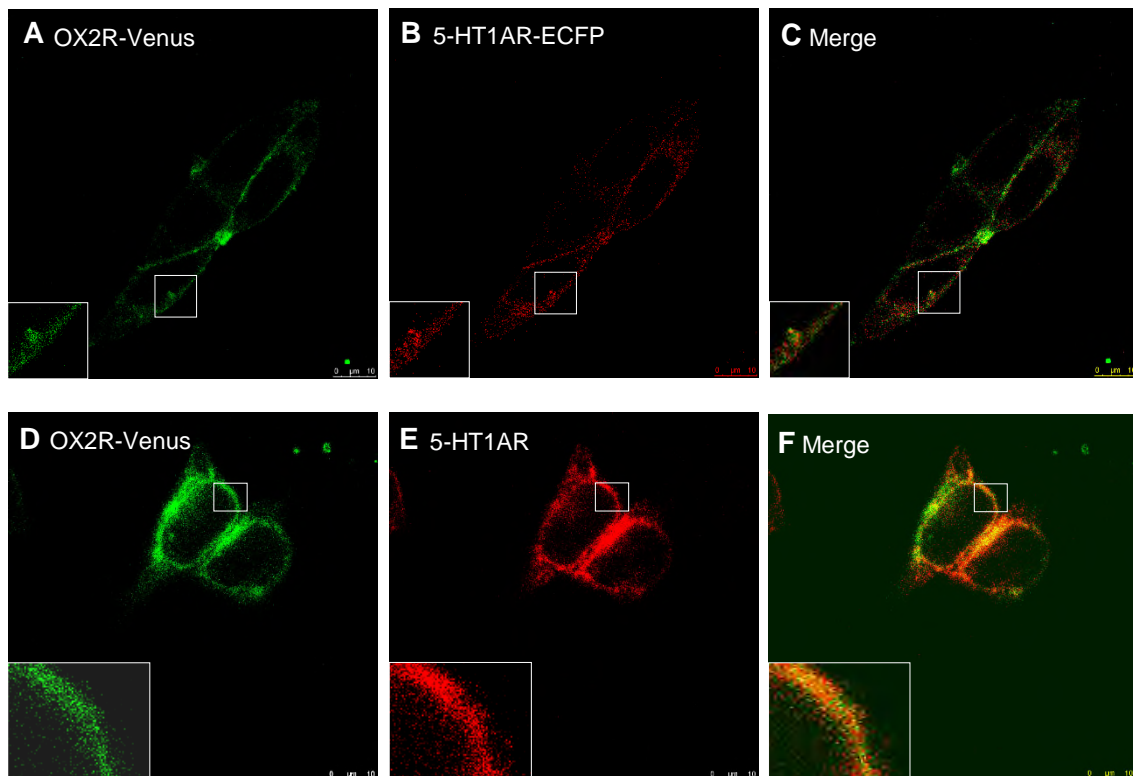
Figure 2. Co-localization of 5-HT1AR and OX2R in the cell membrane of HEK293T cells.
(A-C) Representative photomicrographs showing the co-localization of 5-HT1AR and OX2R in HEK293T cells transfected with OX2R-Venus (green, A) and 5-HT1AR-ECFP (cyan, B). The co-localization was indicated by C.

(D-F) Confocal microscopy image of the co-localization of 5-HT1AR and OX2R in HEK293T cells transfected with 5-HT1AR and OX2R-Venus. OX2R-Venus indicated the expression pattern of OX2R (D). Anti-5-HT1AR antibody was used to indicate the expression pattern of 5-HT1AR (E). The co-localization was indicated by F. Scale bars=10 μm.

## The direct interaction between 5-HT1AR and OX2R in HEK293T cells

BRET assay is very efficient to evaluate the direct interaction of different proteins [26-28]. To further evaluate the existence of 5-HT1AR-OX2R heterodimer, we used BRET analysis to determine whether 5-HT1AR interacted with OX2R directly. 5-HT1AR-Venus and/or OX2R-Rluc plasmids were introduced into HEK293T cells.

For BRET experiment, the substrate coelenterazine H (COH) was added into the medium at the final concentration of 5 μM. Then the 5-HT1AR agonist 8-OHDPAT and/or the OX2R agonist orexin B (OB) were incubated at the final concentration of 3 mg/L (8-OHDPAT) or 0.3 mg/L (OB) respectively. The analysis was performed immediately using the Tristar LB941 plate reader. The data were collected at every 5 mins in duration of 20 mins. And the results showed that the mBRET values were higher in the HEK293T cells with co-transfection of 5-HT1AR-Venus and OX2R-Rluc plasmids compared to the control group in all the indicated periods of detected-time (Figure 3A). Meanwhile, the 5-HT1AR agonist 8-OHDPAT and/or the OX2R agonist OB were added respectively to investigate the role of 5-HT1AR and OX2R activation in regulation of the interaction of these two receptors. As shown in Figure 3B, the mBRET values were potentiated after 8-OHDPAT and/or OB treatment, indicating that the direct interaction of 5-HT1AR and OX2R could be enhanced following activation of the heterodimer. Besides, the direct interaction of the two receptors could also be enhanced in HEK293T cells of transfection of the two factors with the increase of the concentration of the agonists (Figure 3C).

To verify the specificity of the interaction of 5-HT1AR and OX2R, saturation and competitive assays were performed. For saturation experiment, we transfected the HEK293T cells with a constant amount of OX2R-Rluc and the increasing amount of 5-HT1AR-Venus. For competition experiment, a constant amount of 5-HT1AR-Venus and OX2R-Rluc combining with the increasing amount of 5-HT1AR without any tags

were transfected into the HEK293T cells. The empty plasmid pCDNA3.1 was used to keep the constant amount of the total plasmids of every well. The cells were transferred into 96-well microplate 24 h after transfection of the plasmids. The substrate coelenterazine H at the final concentration of 5 μM was added into the medium. The 5-HT1AR agonist 8-OHDPAT and/or the OX2R agonist OB were then added. The analysis was carried out immediately using the Tristar LB941 plate reader. mBRET values were collected to make the saturation and competition curves (Figure 3D-F). The results showed that the mBRET value was elevated in a dose-dependent with the increasing amounts of 5-HT1AR-Venus plasmid and reached a saturation stage when the ratio of the amount of 5-HT1AR-Venus to OX2R-Rluc was 7, indicating that the interaction between 5-HT1AR and OX2R was not due to the overexpression of these two receptors and the interaction between the two receptors was specific (Figure 3D). Consistently, the results from competitive assay showed that the value of mBRET decreased gradually with the increasement of the amount of 5-HT1AR or OX2R with no tags (Figure 3E-F). Together, these results suggested that 5-HT1AR and OX2R directly interacted in HEK293T cells.
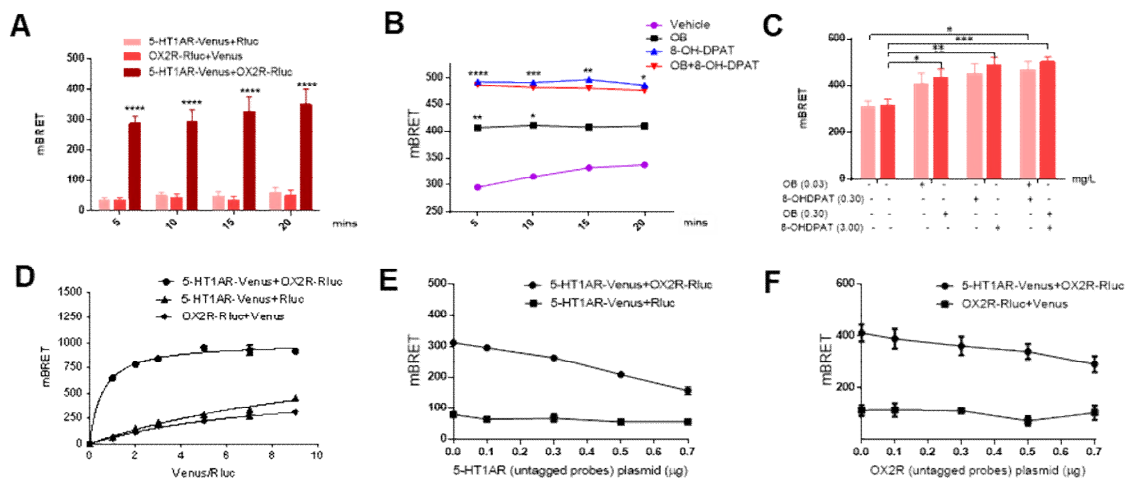
Figure 3. Formation of 5-HT1AR and OX2R heterodimer determined by BRET assay in HEK293T cells.

(A-C) Show the interaction of 5-HT1AR and OX2R in HEK293T cells with co-transfected 5-HT1AR-Venus and OX2R-Rluc without (A) or with the agonist 8-OHDPAT and OB treatment (B-C). P values were obtained by copmaring the "5-HT1AR-Venus and OX2R-Rluc" group to the "5-HT1AR-Venus and Rluc" group in (A). P values were obtained by copmaring the "OB" group or the "8-OHDPAT" group or the "OB+8-OHDPAT" group to the "Vehicle" group in (B).

(D) The saturation curve of the heterodimerization of 5-HT1AR and OX2R. HEK293T cells were

transfected with the constant amount of OX2R-Rluc and the increasing amount of 5-HT1AR-Venus. BRET values were collected at different ratios of the amount of 5-HT1AR-Venus to OX2R-Rluc. All the data were used to make the saturation curve by GraphPad.

(E-F) The competition curve of the heterodimerization of 5-HT1AR and OX2R. HEK293T cells were transfected with the constant amount of OX2R-Rluc and 5-HT1AR-Venus plasmids and the increasing amount of 5-HT1AR (E) or OX2R (F) without any tags.

Data were presented as mean ± S.E.M.. *P < 0.05, ** P < 0.01, *** P < 0.001, **** P < 0.0001.

The co-immunoprecipitation of 5-HT1AR and OX2R

To further confirm the interaction of 5-HT1AR and OX2R, we performed immunoprecipitation experiment. The plasmids of Myc-5-HT1AR and HA-OX2R were co-transfected into HEK293T cells. As shown in Figure 4A and B, the levels of 5-HT1AR and OX2R protein were greatly upregulated in HEK293T cells after the transfection of myc-5-HT1AR and HA-OX2R plasmids (Figure 4A-B). Moreover, the immunoprecipitation results revealed a 5-HT1AR band in the products after pulling-down OX2R by HA antibody (Figure 4C). This finding was highly consistent with the data from PLA and BRET analysis and provided further evidence for the existence of 5-HT1AR-OX2R heterodimers.
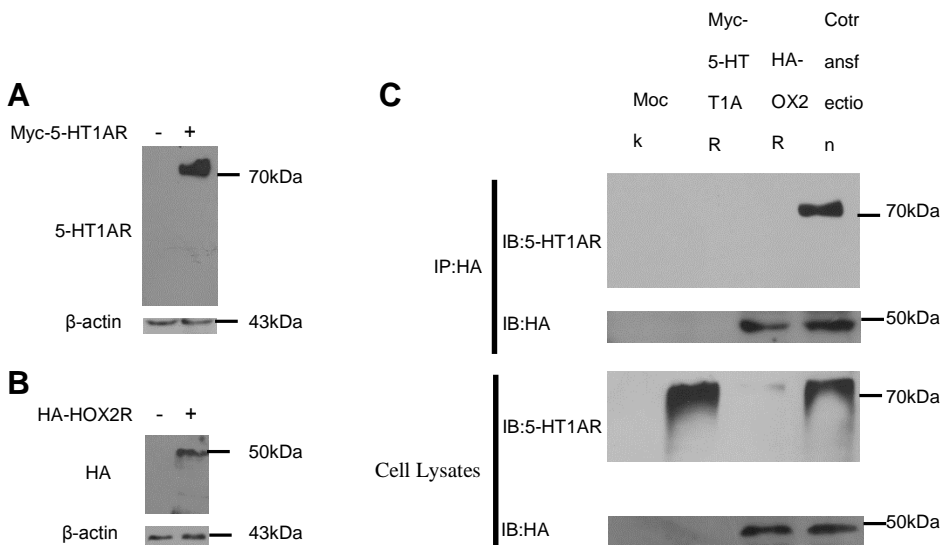
Figure 4. Direct protein-protein interaction of 5-HT1AR and OX2R determined by co-immunoprecipitation assay.

(A) Representative immunoblots of 5-HT1AR and β-actin in HEK293T cells transfected with Myc-5-HT1AR. The 5-HT1AR and β-actin antibodies to evaluate the over expression of 5-HT1AR.

(B) Representative immunoblots of OX2R and β-actin in HEK293T cells transfected with HA-OX2R. The OX2R and β-actin antibodies to evaluate the over expression of OX2R.

(C) Representative immunoblots of immunoprecipites from the total lysates of HEK293T cells transfected with Myc-5-HT1AR or/and HA-OX2R and probed with anti-5-HT1AR or HA.

5-HT1AR-OX2R heterodimer changed the cellular cAMP and calcium levels

Cellular cAMP and calcium were critical in regulating cell viability, inflammatory response, oxidative stress reaction and reward learning in the central nervous system [29-36]. Dysfunction of cellular cAMP and calcium contributed to neurodegenerative and psychiatric disorders [37]. Recent studies indicated the interaction of cAMP and calcium as the potential therapeutic targets for the treatment of neurological diseases [37]. As reported, OX2R activation regulated cellular cAMP and calcium levels [18, 19]. However, 5-HT1AR activation reduced the cellular cAMP levels, while having no effect on calcium influx [10]. Moreover, the heterodimer of different GPCRs led to the changes of levels of cAMP and calcium [10, 38]. To explore whether 5-HT1AR-OX2R heterodimers affected the levels of cAMP and calcium, cAMP BRET biosensor and Fluo-4NW assay kit were performed respectively.

We also investigated the expression levels of 5-HT1AR and OX2R in HEK293T cells after transfection. And the results showed that the expression levels of the two receptors in 5-HT1AR or OX2R group were comparable to that of the co-transfected group (Figure 5A-B). Epac cAMP BRET biosensor consisting of Rluc with Epac tag in the N-terminal and YFP at the C-terminal was effective to detect the cellular cAMP levels. When the levels of cAMP increase, cAMP binds to the Epac resulting in the conformational changes of the sensor, leading to the increase of the distance between YFP and Rluc, and resulting in the decrease of the signals (Figure 5C). The cAMP biosensor YFP-Epac-Rluc and 5-HT1AR or/and OX2R were introduced into HEK293T cells. And the cAMP biosensor YFP-Epac-Rluc alone was introduced into HEK293T cells was as the control group. The cells were transferred into 96-well microplate for BRET experiment. 24 h later, the 5-HT1AR agonist 8-OHDPAT and/or the OX2R agonist OB were added into the medium at the final concentration of 3 mg/L (8-OHDPAT) or 0.3 mg/L (OB) respectively. The data were collected using the

Tristar LB941 plate reader. The results showed that 8-OHDPAT and/or OB treatment alone did not change the basal cAMP levels HEK293T cells. And consistent with the previous findings, the levels of cAMP were reduced by 8-OHDPAT in 5-HT1AR transfected group, while OB treatment increased the levels of cAMP in OX2R transfected group [10]. However, there is no significant difference of cAMP levels in HEK293T-5-HT1AR/OX2R group after 8-OHDPAT or OX2R treatment alone. While the cAMP levels increased significantly in HEK293T-5-HT1AR/OX2R group after both 8-OHDPAT and OB challenge compared with no agonist treatment (Figure 5D). Additionally, the levels of cAMP decreased significantly in HEK293T-5-HT1AR cells after treatment with 8-OHDPAT (Supplementary Figure 1A). While cAMP and calcium levels increased robustly in HEK293T-OX2R cells after treatment with OB (Supplementary Figure 1B). While there were no significant changes of cAMP and calcium after treatment with different concentrations of 8-OHDPAT or OB in HEK293T-5-HT1AR group and HEK293T-5-OX2R group (Supplementary Figure 1A-B). Besides, the cAMP levels increased significantly in HEK293T-5-HT1AR/OX2R group after treatment with 8-OHDPAT and OB compared with the untreated group (Supplementary Figure 1C). Additionally, the upregulation of cAMP depended on the concentrations of 8-OHDPAT and OB (Supplementary Figure 1C). These results suggested that the 5-HT1AR-OX2R heterodimer affected the levels of cellular cAMP in a new way which was different from the monomers of 5-HT1AR or OX2R (Figure 5D).

Fluo-4NW is a calcium indicator and Fluo-4NW kit has been taken as the effective and convenient way to evaluate the levels of cellular calcium. The results of Fluo-4NW assay demonstrated that 8-OHDPAT treatment had no effect on the calcium levels in 5-HT1AR group, while OB challenge increased the levels of calcium in OX2R group (Figure 5E). 8-OHDPAT treatment had no effect on the calcium levels in HEK293T-5-HT1AR/OX2R group compared to the 5-HT1AR group with 8-OHDPAT treatment (Figure 5E). However, the levels of calcium increased robustly of HEK293T-5-HT1AR/OX2R group after 8-OHDPAT and OB challenge compared with the 5-HT1AR group with 8-OHDPAT treatment, and lower than that of

the OX2R transfected group with OB treatment (Figure 5E). Taken together, these results above demonstrated that 5-HT1AR-OX2R heterodimers function as a new receptor which was different from the original 5-HT1AR or OX2R receptor in regulation of cellular calcium levels, which providing new insights into the understanding of the role of 5-HT1AR and OX2R (Figure 5E).
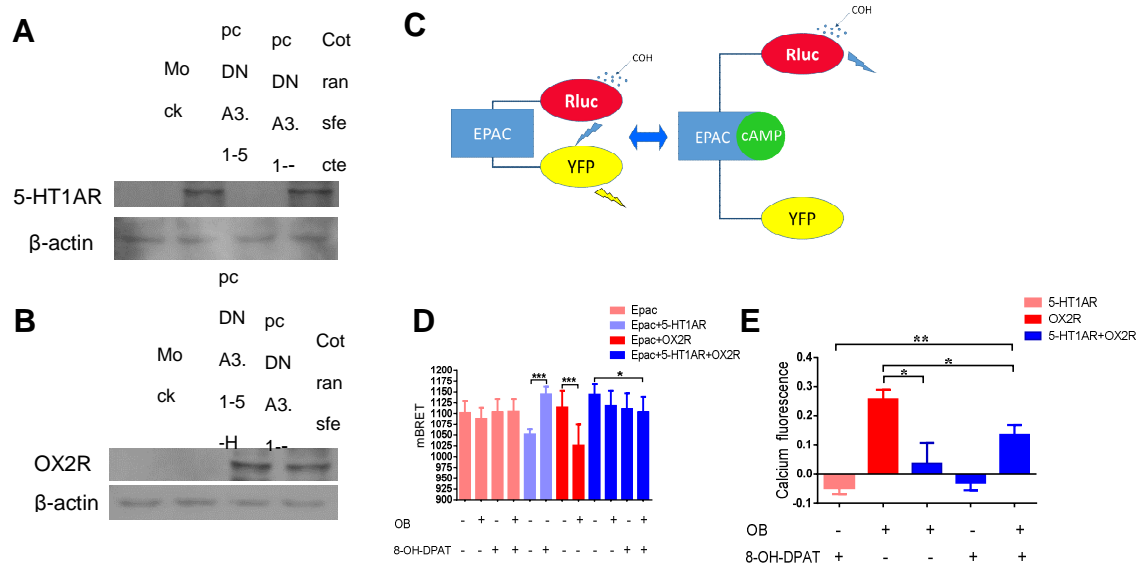
Figure 5 Evaluation of cellular cAMP and calcium levels by 5-HT1AR-OX2R heterodimer activation.

(A-B) Representative immunoblots of the total lysates of HEK293T cells transfected with 5-HT1AR or/and OX2R and probed with anti-5-HT1AR (A) or OX2R (B).

(C) Show the schematic diagram of the EPAC BRET biosensor.

(D) Show the cellular cAMP levels in HEK293T cells transfected with 5-HT1AR and/or OX2R using EPAC BRET biosensor.

(E) Show the cellular calcium levels HEK293T cells transfected with 5-HT1AR and/or OX2R using Fluo-4NW assay kit.

Data were expressed as mean ± S.E.M. *P < 0.05, ** P < 0.01, *** P < 0.01.

5-HT1AR-OX2R heterodimer downregulated p-ERK levels

As one member of mitogen-activated protein kinases (MAPK) family, extracellular signal-related kinase (ERK) plays vital roles in cell migration, cell proliferation, cell differentiation and apoptosis [39]. Early studies showed that enhancement of p-ERK protected dopaminergic neurons in substantia nigra from death caused by neurotoxin MPTP [40], indicating the important role of ERK in brain disorders. Moreover, previous research demonstrated that both 5-HT1AR and OX2R regulated the levels of

p-ERK [15, 20].

We then investigated whether the heterodimer of 5-HT1AR and OX2R would affect the levels of ERK and p-ERK. Western blotting was performed to determine the levels of total ERK and p-ERK of 5-HT1AR-OX2R heterodimers after agonist stimulation. The results showed that there was no difference of the levels of total ERK after agonist challenge among HEK293T-5-HT1AR group, HEK293T-OX2R group and HEK293T-5-HT1AR/OX2R group (Figure 6A-F). However, the levels of p-ERK increased approximately four folds 5 mins after 8-OHDPAT challenge and reached the peak at 30 mins in HEK293T-5-HT1AR group (Figure 6A). The levels of p-ERK increased approximately two folds 5 mins after OB challenge and reached the peak at 15 mins in HEK293T-OX2R group (Figure 6B). Moreover, the levels of p-ERK increased significantly 5 mins in HEK293T-5-HT1AR/OX2R group after both 8-OHDPAT and OB treatment. However, there was no change of p-ERK levels from 15 to 60 mins in HEK293T-5-HT1AR/OX2R group after the 8-OHDPAT and OB treatment (Figure 6 C). Besides, the levels of p-ERK levels in HEK293T-5-HT1AR group were increased gradually 10 mins after treatment with the increasement of the concentration of 8-OHDPAT (Figure 7A). Also, the levels of p-ERK levels of HEK293T-OX2R cells were increased gradually 10 mins after treatment with the increase of the concentration of OB (Figure 7B). While there was an increase trend of the levels of p-ERK in HEK293T-OX2R group after treatment with different concentrations of 8-OHDPAT and OB (Figure 7C). The statistical data also confirmed the results (Figure 7D-F). Additionally, the results of further experiments showed that there were no significant changes of p-ERK levels in HEK293T-HT1AR/OX2R group 10 mins following treatment with 8-OHPAT or OB compared with the untreated group (Supplementary Figure 2A-B), indicating that the 5-HT1AR-OX2R heterodimers functioned in a way which was different from the original receptors. Altogether, these findings demonstrated that the expression levels of p-ERK decreased in HEK293T-5-HT1AR/OX2R group compared with HEK293T-5-HT1AR or HEK293T-OX2R group following agonist challenge (Figure 6-7).
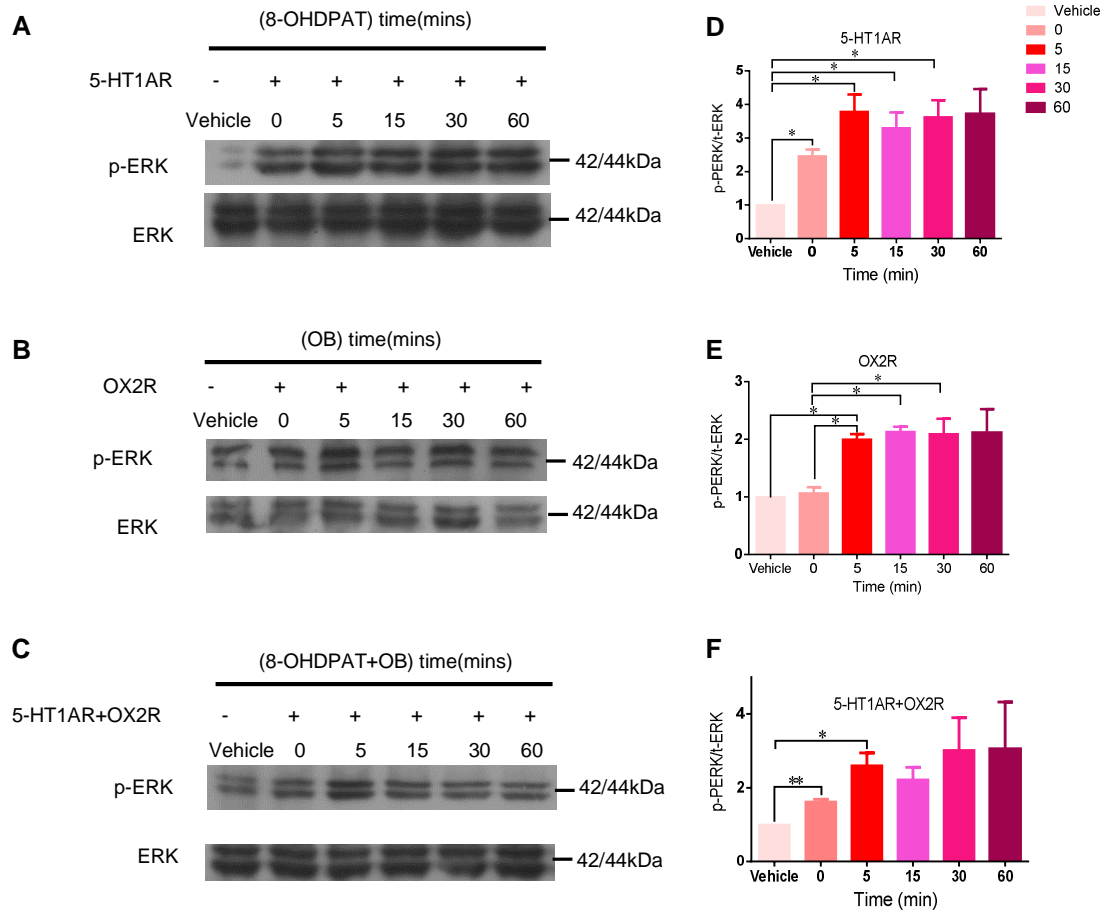
Figure 6. The heterodimer of 5-HT1AR and OX2R downregulated the phosphorylation of ERK.

(A) Representative immunoblots of p-ERK in HEK293T cells transfected with 5-HT1AR following 8-OHDPAT treatment.

(B) Representative immunoblots of p-ERK in HEK293T cells transfected with OX2R after OB stimulation.
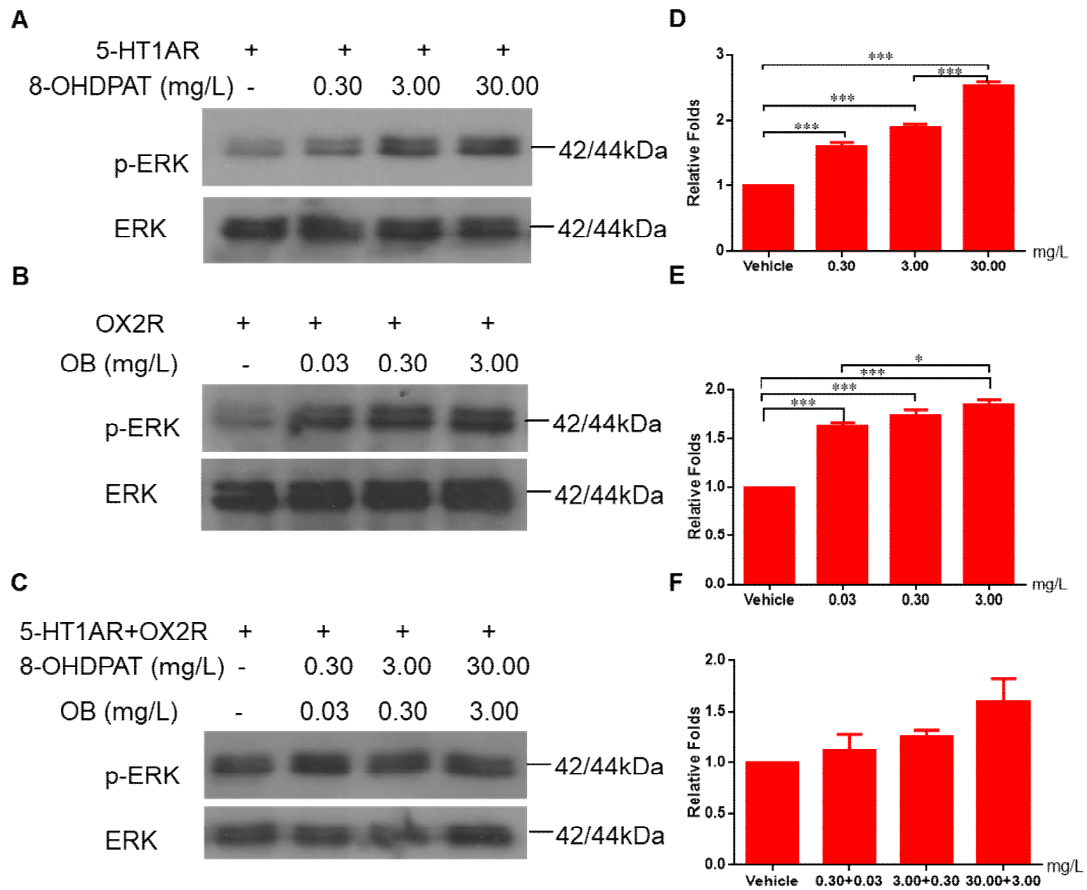
(C) Representative immunoblots of p-ERK in HEK293T cells transfected with 5-HT1AR and OX2R after 8-OHDPAT and OB challenge by western blotting.

(D) Statistics for p-ERK expression in (A).

(E) Statistics for p-ERK expression in (B).

(F) Statistics for p-ERK expression in (C).

Data were expressed as mean ± S.E.M.. *$P < 0.05$, ** $P < 0.01$, *** $P < 0.01$.

Figure 7. The effect of concentrations of 8-OHFPAT and OB on levels of the phosphorylation of ERK.

(A) Representative immunoblots of p-ERK in HEK293T cells transfected with 5-HT1AR following 8-OHDPAT treatment with different concentrations.

(B) Representative immunoblots of p-ERK in HEK293T cells transfected with OX2R after OB stimulation with different concentrations.

(C) Representative immunoblots of p-ERK in HEK293T cells transfected with 5-HT1AR and OX2R after 8-OHDPAT and OB challenge with different concentrations.

(D) Statistics for p-ERK expression in (A).

(E) Statistics for p-ERK expression in (B).

(F) Statistics for p-ERK expression in (C).

Data were expressed as mean ± S.E.M. *$P < 0.05$, ** $P < 0.01$, *** $P < 0.01$.

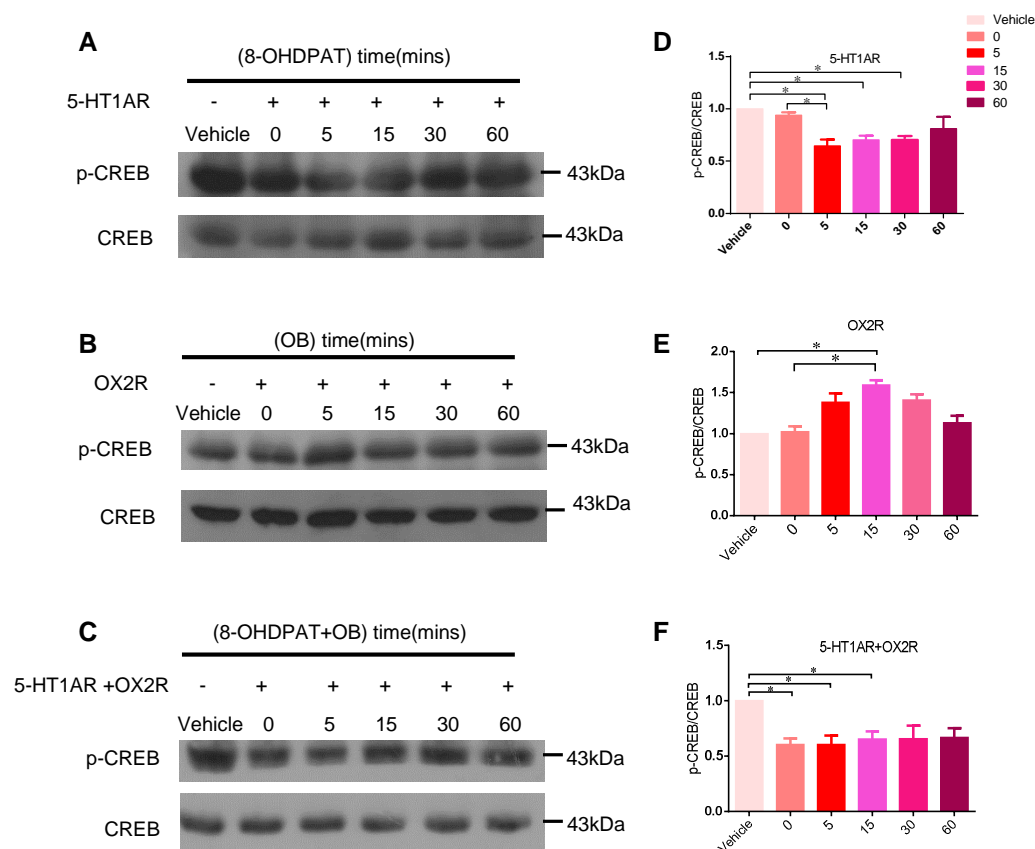## 5-HT1AR-OX2R heterodimer downregulated p-CREB levels

CREB plays important roles in the maintenance of immune homeostasis and regulating of learning and memory in the central nervous system [41, 42]. It has been reported that the behavior and cognition ability of mice is regulated by CREB in hippocampus, indicating the essential role of CREB for hippocampus function [43].

Defect of CREB contributed to the progresses of brain disorders such as depression [44]. Previous studies revealed that GPCR induced the upregulation of phosphorylated CREB (p-CREB) through enhancing the activation of adenylyl cyclase (AC). While the levels of p-CREB decreased when GPCR coupling to the Gi protein causing the reduction of the activation of adenylyl cyclase (AC) [45]. Additionally, as the Gi-coupled GPCR, 5-HT1AR has been reported to reduce p-CREB levels after 8-OHDPAT stimulation [10, 45]. To uncover whether 5-HT1AR-OX2R heterodimers affect the levels of p-CREB, western blotting was performed to determine the expression levels of total CREB and p-CREB of 5-HT1AR-OX2R heterodimers after agonist challenge. The results showed that there was no difference in the levels of total CREB among HEK293T-5-HT1AR group, HEK293T-OX2R group and HEK293T-5-HT1AR/OX2R group (Figure 8A-F). However, the levels of p-CREB decreased significantly in HEK293T-5-HT1AR/OX2R group compared with HEK293T-5-HT1AR or HEK293T-OX2R group without agonist treatment (Figure 8A-C). Furthermore, the expression levels of p-CREB in HEK293T-5-HT1AR/OX2R group tended to decrease after the treatment of 8-PHDPAT and OB (Figure 8C). Additionally, the levels of p-CREB in HEK293T-5-HT1AR group were decreased gradually 10 mins after treatment with the increase of the concentration of 8-OHDPAT (Figure 9A). While the levels of p-CREB HEK293T-OX2R group were increased gradually 10 mins after treatment with the increase of the concentration of OB (Figure 9B). And the levels of p-CREB in HEK293T-5-HT1AR/OX2R group decreased significantly after treatment with high concentration of 8-OHDPAT and OB compared with the untreated group (Figure 9C). The statistical data also confirmed the results (Figure 9D-F). Therefore, all these results demonstrated that the expression levels of p-CREB decreased in HEK293T-5-HT1AR/OX2R group compared with HEK293T-5-HT1AR or HEK293T-OX2R group after agonist treatment (Figure 8-9).

Taken together, our findings demonstrated that 5-HT1AR and OX2R formed the heterodimers and affected downstream signaling molecular which was different from monomers of 5-HT1AR or OX2R (Figure 10).

Figure 8. The heterodimer of 5-HT1AR and OX2R downregulated the phosphorylation of p-CREB.

(A)Representative immunoblots of p-CREB in HEK293T cells transfected with 5-HT1AR following 8-OHDPAT treatment.

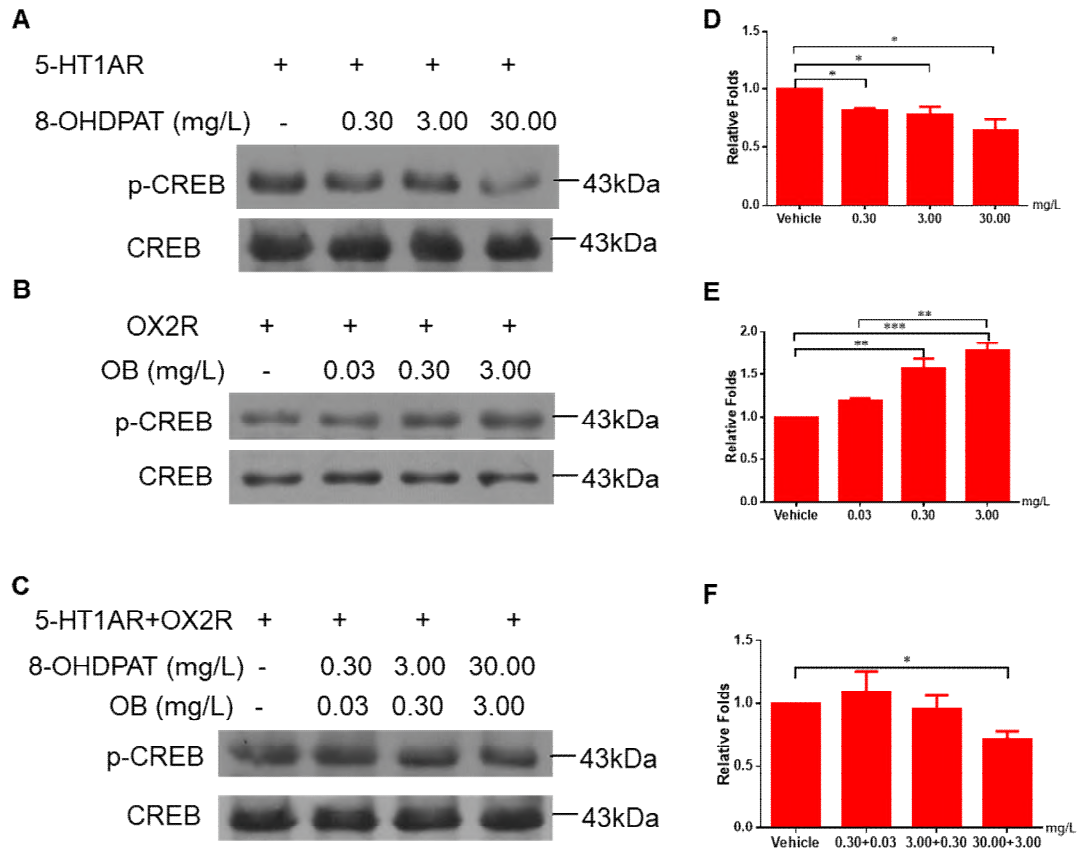(B)Representative immunoblots of p-CREB in HEK293T cells transfected with OX2R after OB stimulation.

(C)Representative immunoblots of p-CREB in HEK293T cells transfected with 5-HT1AR and OX2R after 8-OHDPAT and OB challenge.

(D)Statistics for p-CREB expression in (A).

(E) Statistics for p-CREB expression in (B).

(F) Statistics for p-CREB expression in (C).

Data were expressed as mean ± S.E.M.. *$P < 0.05$, ** $P < 0.01$, *** $P < 0.01$.

Figure 9. The effect of concentrations of 8-OHFPAT and OB on levels of the phosphorylation of CREB.

(A) Representative immunoblots of p-CREB in HEK293T cells transfected with 5-HT1AR following 8-OHDPAT treatment with different concentrations.

(B) Representative immunoblots of p-CREB in HEK293T cells transfected with OX2R after OB stimulation with different concentrations.

(C) Representative immunoblots of p-CREB in HEK293T cells transfected with 5-HT1AR and OX2R after 8-OHDPAT and OB challenge with different concentrations.

(D) Statistics for p-CREB expression in (A).

(E) Statistics for p-CREB expression in (B).

(F) Statistics for p-CREB expression in (C).

Data were expressed as mean ± S.E.M. *$P < 0.05$, ** $P < 0.01$, *** $P < 0.01$.

Discussion

In the present study, we found the heterodimer formation of 5-HT1AR and OX2R and the heterodimer affected the downstream signaling. Firstly, the formation of 5-HT1AR-OX2R heterodimer was observed in hippocampus of adult rat by PLA. Secondly, immunofluorescence analysis showed 5-HT1AR and OX2R were

co-localized in HEK293T cells. BRET assay results revealed the heterodimer formation of 5-HT1AR-OX2R and the agonist treatment enhanced the direct-direct interaction of the two receptors. Thirdly, co-immunoprecipation experiment further demonstrated the protein direct-direct interaction between 5-HT1AR and OX2R, which was consistence with the results of BRET assay. Lastly, compared to the 5-HT1AR transfected group after 8-OHDPAT stimulation, western blotting displayed that the levels of cellular calcium and cAMP were upregulated significantly and the expression levels of p-CREB and p-ERK were downregulated in the HEK293T-5-HT1AR/OX2R group following 8-OHDPAT and OB treatment. Altogether, these findings provided direct evidence of the formation of 5-HT1AR-OX2R heterodimer and highlight the potential role of the heterodimer in physiological and pathological conditions in the central nervous system (Figure 10).
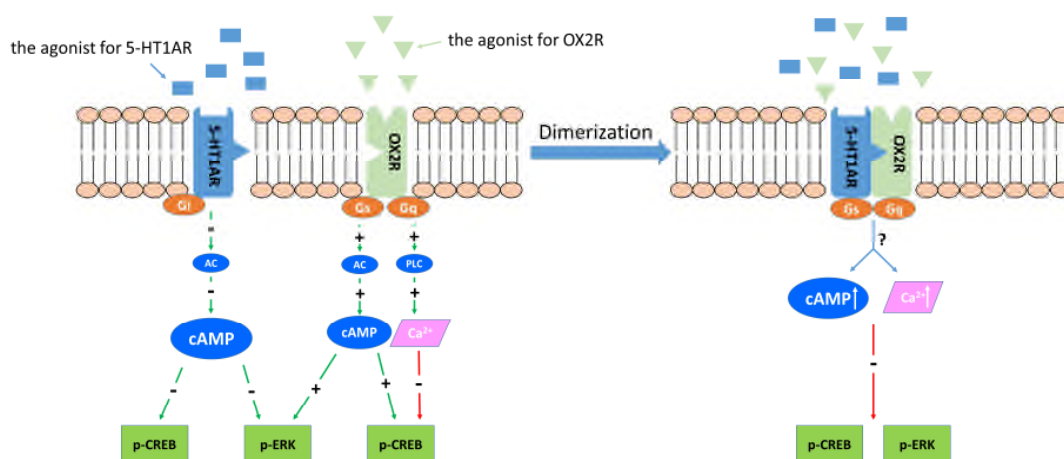
Figure 10. The schematic representation of 5-HT1AR-OX2R heterodimer-induced downstream signaling.
The heterodimer of 5-HT1AR and OX2R significantly upregulated the levels of cellular cAMP and calcium, and downregulated the levels of p-ERK and p-CREB after activation by the agonists.

The homodimer or the heterodimer of GPCRs have been studied for many years [38, 46]. As members of GPCRs, 5-HT1AR and OX2R are both widely expressed in hippocampus [13, 17]. Given the similar localization and characteristics of 5-HT1AR and OX2R in brain, 5-HT1AR and OX2R probably form heterodimer in the central nervous system. As the results shown above, we firstly confirmed the formation of

5-HT1AR and OX2R by PLA. PLA assay has been reported to be a very efficient method to detect the direct interaction between different proteins[47]. And our PLA data demonstrated that 5-HT1AR and OX2R formed heterodimers in hippocampus (Figure 1A-G). Additionally, we also found that there were very few PLA dots in cortex. The different pattern of the PLA data in different brain areas probably resulted from the distinct expression pattern and different functions of the two receptors in various brain regions.

Considerable studies showed that the heterodimers formed by different GPCRs could affect the downstream signaling pathway [47-49]. In our current study, we also explored the signaling transduction affected by 5-HT1AR-OX2R heterodimer using cAMP BRET biosensor, Fluo-4NW kit and western blotting analysis. The levels of cellular cAMP and calcium increased robustly of HEK293T-5-HT1AR/OX2R group following 8-OHDPAT and OB challenge, indicating the heterodimer of 5-HT1AR-OX2R affect the expression levels of the second messengers. ERK and CREB were the key molecules downstream of 5-HT1AR and OX2R. In addition to the involvement in physiological processes including cell proliferation, cell migration and memory [50-54], ERK and CREB also play important roles in pathological processes including hyperalgesia, ischemic stroke, Alzheimer's disease and pain [55-58]. As described above, 5-HT1AR has been reported to decrease the levels of cAMP, leading to the downregulation of p-CREB after ligand stimulation. In contrast, OX2R induced the upregulation of cAMP levels, leading to the increasement of p-CREB after OB stimulation. Our results revealed that 5-HT1AR-OX2R heterodimer induced the downregulation of p-ERK and p-CREB after 8-OHDPAT and OB challenge compared with the 5-HT1AR transfected group treated with 8-OHDPAT. Interestingly, the expression level of p-CREB decreased significantly in HEK293T cells with overexpression of 5-HT1AR and OX2R compared with the control group (Figure 8-9). And the levels of p-CREB in HEK293T-5-HT1AR/OX2R group tend to further decrease after the challenge of 8-OHDPAT and OB (Figure 8-9). These results suggested that the 5-HT1AR and OX2R heterodimer regulated the expression levels of p-CREB.

The results above indicated that 5-HT1AR-OX2R heterodimer affected the downstream signaling transduction and the expression levels of cellular molecules including calcium, cAMP, p-ERK and p-CREB (Figure 5-9). The mechanism underlying this regulation remains unclear. Several suggestions from the above results are listed as below. On one hand, the heterodimer of 5-HT1AR and OX2R as a novel receptor, which was different from original 5-HT1AR or OX2R, induced the downstream signaling after co-activation by 8-OHDPAT and OB. On the other hand, as described above, the heterodimer of 5-HT1AR and OX2R in HEK293T cells led to the upregulation of cAMP and calcium after 8-OHDPAT and OB stimulation compared to the 5-HT1AR group following 8-OHDPAT stimulation (Figure 5C-E). It was noteworthy that the increasement of calcium levels in the co-transfected group treated with 8-OHDPAT and OB was still lower than OX2R group after OB treatment, while 5-HT1AR alone induced the downregulation of cAMP and no changes of calcium levels after ligand treatment (Figure 5C-E). 5-HT1AR and OX2R heterodimer led to the downregulation of cellular p-ERK and p-CREB compared to the OX2R group after OB stimulation. Here, we found 5-HT1AR downregulated the levels of p-CREB and OX2R upregulated the levels of p-CREB (Figure 8A-B). Activation of 5-HT1AR-OX2R heterodimers induced the upregulation of cAMP, while leading to the downregulation of p-CREB (Figure 5D and Figure 8). As mentioned above, 5-HT1AR mainly binds to the Gi protein, leading to the decrease of adenylate cyclase (AC) activation, and further leads to the downregulation of levels of p-CREB and cellular cAMP after ligand stimulation [15]. And OX2R mainly binds to the Gs protein and Gq protein resulting in the activation of adenylate cyclase (AC), and further leads to the upregulation of the expression levels of p-CREB, p-ERK, cellular cAMP and calcium levels after ligand stimulation [18-20]. In the study, we found activation of 5-HT1AR-OX2R heterodimers increased the levels of cAMP and calcium, also led to the downregulation of p-ERK and p-CREB (Figure 6 and Figure 8). Thus, the signaling changes of the heterodimers after ligand treatment might result from the activation of Gs and Gq signaling, which would cause the upregulation of cAMP and calcium. Additionally, it has been reported cAMP induced the upregulation

of p-CREB by activating protein kinase A (PKA). And calcium had positive effects on the expression levels of p-CREB through regulating calmodulin-dependent kinases (CaMK) [59]. Besides, the signaling pathway of cAMP could be regulated by CaMK and mitogen-activated protein kinase (MAPK) [59]. Thus, the downregulation of p-CREB in 5-HT1AR/OX2R group after ligands stimulation might result from increasement of cAMP and calcium levels.

cAMP/PKA pathway was a very important regulator of neurodegeneration, learning and memory [60]. Previous studies showed that enhancement of calcium-CREB signaling pathway improved the ability of learning and memory of rats [61]. Additionally, the results from a genome-wide association study demonstrated that CREB interacting with some of risk genes of mental disorders, suggesting that CREB probably be identified as one of the risk factors for psychiatric disorders including schizophrenia and major depression disorder [62]. Besides, enhancement of p-ERK/p-CREB signaling ameliorated the death of dopaminergic cell line SH-SY5Y cells after neurotoxin MPP$^+$ challenge and dopaminergic neurons in *substantia nigra* (SN) by neurotoxin MPTP treatment [40, 63]. Together, these findings revealed that cAMP-calcium-ERK-CREB signaling was a very important regulator of neurological disease. Importantly, the expression levels of 5-HT1AR decreased significantly in depression model [64]. And OX2R knockout mice presented as an increase of despair, indicating the important role of OX2R in mental disorders such as depression [25]. Our data revealed that the heterodimer of 5-HT1AR and OX2R modulated cAMP-calcium-ERK-CREB pathway, which providing a new therapeutic target for neurological diseases.

As a GPCR, 5-HT1AR forms heterodimer with other GPCRs involved in the regulation of hippocampus neurogenesis [16, 65]. Deficiency of hippocampus neurogenesis has been observed in neurological diseases such as depression and Alzheimer's disease [5, 66], indicating the important role of neurogenesis of hippocampus in the brain. 5-HT1AR has been reported to regulate the neurogenesis of hippocampus [67, 68]. Moreover, lines of evidence showed that 5-HT1AR was involved in the pathology of neurological diseases such as Parkinson's disease and

depression [64, 69-73]. Recent research demonstrated that 5-HT1AR and FGFR1 formed heterodimer and enhanced the plasticity of hippocampal neurons [16]. Interestingly, intracerebroventricular co-injection of 8-OHDPAT and FGF2 resulted in reduction in immobility and increased swimming time of adult rats compared with the vehicle group or 8-OHDPAT group or FGF2 group, indicating the potential role of heterodimer of 5-HT1AR with other GPCRs as the therapeutic targets for depression [16]. Thus, further animal experiments and clinical analyses are needed to uncover the function of the 5-HT1AR-OX2R heterodimer in the regulation of plasticity of hippocampus. OX2R has been reported to be involved in the processes of depression. OX2R deficiency enhanced the symptom of despair, indicating that OX2R might have good effects on depression [25]. As described above, 5-HT1AR was also participated in the pathology of depression. Behavior test revealed that the upregulation of 5-HT1AR expression improved the performance of depressed rats [74]. This data suggested that 5-HT1AR had beneficial effects on depression. Herein, we found the formation of 5-HT1AR and OX2R heterodimer, which functioned in a different way from 5-HT1AR or OX2R alone, indicating the potential roles of the 5-HT1AR-OX2R heterodimer in the central nervous system.
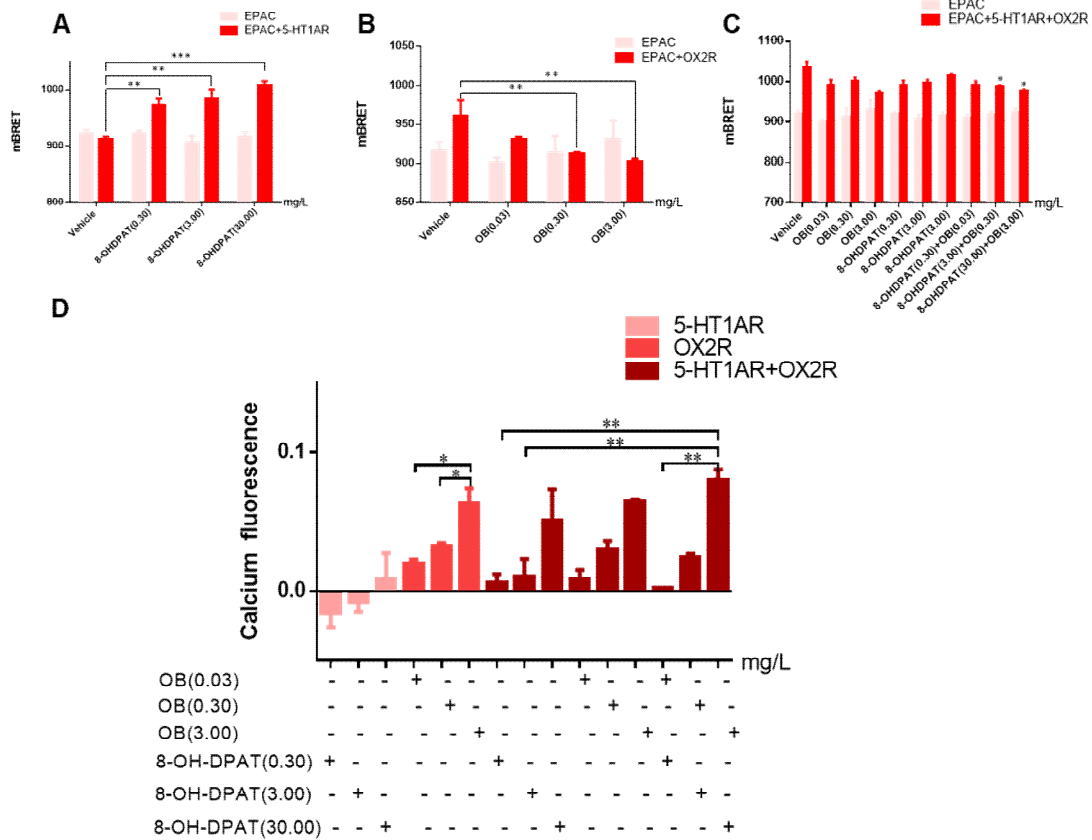
Supplementary Figure 1. Levels of cAMP and calcium in HEK293T-5-HT1AR-OX2R cells after treatment with different concentration of 8-OHDPAT and OB.

(A-C) Show the cellular cAMP levels in   HEK293T cells transfected with 5-HT1AR (A) or OX2R (B) or 5-HT1AR/OX2R (C) using EPAC BRET biosensor following 8-OHDPAT and/or OB treatment with different concentrations.

(D) Show the cellular calcium levels HEK293T cells transfected with 5-HT1AR and/or OX2R using Fluo-4NW assay kit following 8-OHDPAT and/or OB treatment with different concentrations..

Data were expressed as mean ± S.E.M. *P < 0.05, ** P < 0.01, *** P < 0.01.

A

B
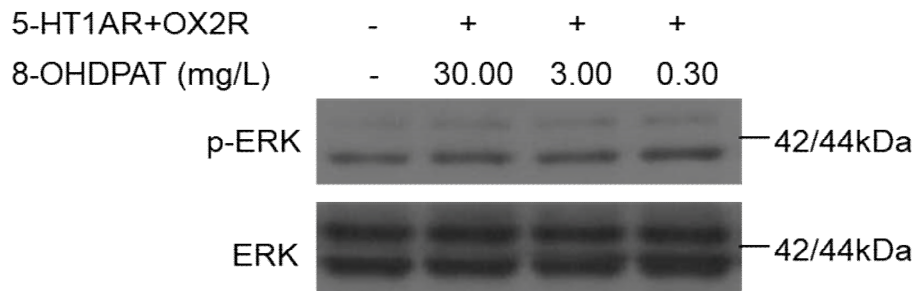
Supplementary Figure 2. Evaluation of cellular p-ERK levels by 5-HT1AR-OX2R heterodimer activation in HEK293T cells treated with 8-OHDPAT or OB.

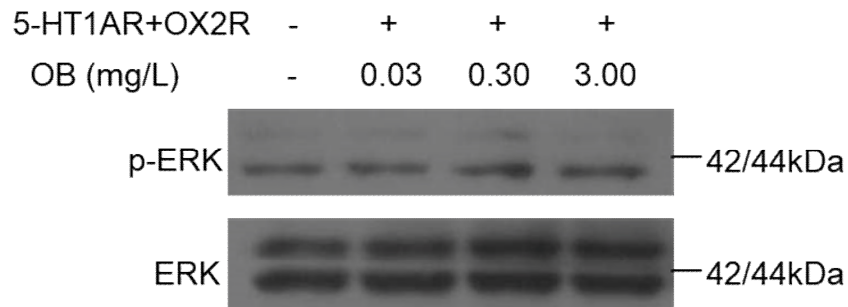(A) Show the cellular p-ERK levels in HEK293T cells transfected with 5-HT1AR and OX2R following treatment with 8-OHDPAT of different concentrations.

(B) Show the cellular p-ERK levels in HEK293T cells transfected with 5-HT1AR and OX2R following treatment with OB of different concentrations.

Materials and methods

Peptides, regents and antibodies

Human orexin B was purchased from Phoenix Pharmaceuticals (003-31). The 5HT1AR agonist 8-OHDPAT was obtained from sigma (H8520) and the Duolink PLA kit was obtained from Sigma (Duolink In Situ Detection Reagents Red). The transfection regent Lipofectamine^{TM}2000 was purchased from Invitrogen (11668-019). Anti-CREB and anti-phospho-CREB antibodies were purchased from Cell Signaling Technology (anti-CREB antibody:9197, anti-p-CREB antibody:9198). Anti-HA antibody was purchased from Cell Signaling Technology (#3724). Anti-Myc antibody was purchased from Cell Signaling Technology (#2278). Anti-OX2R antibody was

obtained from Merck Millipore (AB3094). Anti-5-HT1AR antibody for western blotting and immunofluorescence was purchased from Cell Signaling Technology (#9897). Anti-5-HT1AR antibody for PLA was obtained from Sigma (SAB2501759). Anti-β-actin antibody was purchased from ZSGB-BIO (TA-09). Anti-p-ERK antibody was obtained from Cell Signaling Technology (#9101). Anti-ERK antibody was purchased from Cell Signaling Technology (#4696).

Plasmid constructs

For immunoprecipitation, a full-length human 5-HT1AR (Gene ID: 3350) was subcloned into the mammalian expression vector pcDNA3.1-Myc-His A using Xha□ and EcoR□. A full-length human OX2R (Gene ID: 3062) was subcloned into the expression vector pcDNA3.1-3HA using Xho□ and Kpn□. pcDNA3.1-Myc-His A, pcDNA3.1-OX2R, pcDNA3.1-5-HT1AR and pcDNA3.1-3HA were gifts from Dr. Chen Jing (Division of Biomedical Sciences, Warwick Medical School, University of Warwick, Coventry, CV4 7AL, UK). For immunofluorescence and BRET, a full-length human 5-HT1AR was subcloned into the N-terminus of pECFP-N1 (Clontech, #6900-1) using Hind□ and BamH□. The OX2R-Rluc plasmid was constructed by subcloning the coding sequence of human OX2R without the stop codon into pRluc-N1 (BioSignal Packard, Inc., Montreal, Canada). Human OX2R was inserted into the N-terminus of pVenus-N1 (Addgene, #61854) using Hind□ and BamH□.

Immunofluorescence

Immunofluorescence analysis was carried out as described previously [75]. In brief, cell cultures were fixed by paraformaldehyde (PFA) for 10 mins and blocked for 2 h in blocking solution at room temperature following by primary antibody incubation overnight at 4□. The samples were washed three times with phosphate-buffered saline (PBS) and then incubated with the secondary antibody for 1 h at room temperature. The secondary antibody used as follows: CY3-conjugated goat anti-rabbit IgG (BOSTER, BA1032, 1:400). Immunosignals were detected and analyzed using a

Leica DMRE laser scanning confocal microscope at the 550nm (Lecia, Milton Keynes, UK). Besides, the Venus signal was collected at the 480 nm. The pixel size of the imaging was 1024× 1024.

Western blotting and Quantification

The procedure of western blotting was according to the instructions described before [47]. Briefly, HEK293T cells expressing 5-HT1AR and/or OX2R were lysed in RIPA (50Mm Tris (PH 7.4), 150Mm NaCl, 1% Triton X-100, 1% sodium deoxycholate, 0.1% SDS) and the proteins extracted with different molecular weights were separated by SDS-PAGE gels. The proteins were then transferred to the PVDF membranes. The membranes were incubated with the primary antibodies overnight at 4□ after blocking with 5% nonfat milk for 2 h at room temperature. The primary antibodies used as follows: Myc (1:1000), HA (1:1000), 5-HT1AR (1:2000), CREB (1:1000), p-CREB (1:1000), ERK (1:1000), p-ERK (1:1000), β-actin (1:5000). The next day, membranes were incubated with the corresponding secondary antibodies for 1 h at room temperature after washing with TBST for 3 times. The secondly antibodies were used as follows: HRP-conjugated goat anti-mouse IgG (1:10000, ZSGB-BIO, ZB-2305), HRP-conjugated goat anti-rabbit IgG (1:10000, ZSGB-BIO, ZB-2301). Peroxidase activity was determined with the chemiluminescent substrate (Multi Sciences, P1425). The band of β-actin was considered as the loading control.

BRET assay for analysis of the interaction of 5-HT1AR and OX2R

BRET assay was performed according to the procedures described previously [47]. The 5-HT1AR-Venus and/or OX2R-Rluc were introduced into HEK293T cells. After 24 h transfection, cells were digested in 0.02% trypsin and plated into a 96-well microplate (Corning 3600) for another 24 h. The substrate coelenterazine H was added into the medium at the final concentration of 5 μM. The 5-HT1AR agonist 8-OHDPAT or the OX2R agonist OB was then added at the final concentration of 3 mg/L or 0.3 mg/L respectively. The analysis was performed immediately using the

Tristar LB941 plate reader (Berthold Technologies, Bad Wildbad, Germany) and the time of duration was under 30 mins because of the activity of the substrate. And the filtered light emission was sequentially recorded at 460 nm and 535 nm respectively by MikroWin 2000 software. The data were presented as "BRET ratio" or "mBRET" (mBRET=1000 × BRET ratio). The value of mBRET was calculated through subtracting the ratio of the control group.

For saturation experiment, we transfected the HEK293T cells in 12-well plate with a constant amount of OX2R-Rluc and the increasing amount of 5-HT1AR-Venus. The empty plasmid pCDNA3.1 was used to keep the constant amount of the total plasmid of each well. mBRET values were collected at different ration of 5-HT1AR-Venus to OX2R-Rluc to plot the saturation curves.

For competition experiment, we transfected the HEK293T cells in 12-well plate with a constant amount of 5-HT1AR-Venus and OX2R-Rluc. Besides, the increasing amount of 5-HT1AR without any tags was added to the reaction system to compete with 5-HT1AR-Venus. And the empty plasmid pCDNA3.1 was also added to keep the constant amount of the total plasmid of each well. mBRET values were collected to plot the competition curves.

Co-immunoprecipitation

To analyze the interaction between 5-HT1AR and OX2R, co-immunoprecipitation assay was performed according to the protocol of Pierce Anti-HA-Agarose (Thermo Scientific, 26181). In brief, approximately 5×10^6 HEK293T cells were harvested after myc-5-HT1AR and/or HA-OX2R transfection for 24 h. The cells were lysed in 150 μl of RIPA buffer. And the supernatant was collected after centrifugation at 12000 g for 15 mins. The pellet resin was then obtained using the 50 μl of Pierce Anti-HA Agarose by centrifugation at 12000 g for 5 seconds. Add 50 μl of the supernatant into the collected pellet resin at a final volume of 200 μl by adding TBS followed by incubation on a rocking platform overnight at 4□. Next day, after centrifugation at 12000 g for 10 seconds, the supernatant was collected and washed with TBST for

three times. Finally, the immunoprecipitation products were analyzed by western blotting.

PLA

The standard procedure for PLA was described before [47]. Briefly, 5 μm paraffin-embedded slices were incubated with anti-5-HT1AR and anti-OX2R antibodies overnight at 4□ after blocked with the blocking solution for 1 h at room temperature. The slices were incubated with plus and minus probes for 1 h at 37□ after washed with Buffer A for three times. The slices were then incubated with the amplification-polymerase solution at 37□ for 3 h. The signals were analyzed by the Leika TCS SP5.

BRET measurement for cAMP

The measurement for cAMP using Epac cAMP BRET biosensor analysis was according to the procedures described previously [47, 76]. In brief, HEK293T cells were transfected with the cAMP biosensor YFP-Epac-Rluc. And the cAMP biosensor YFP-Epac-Rluc alone was transfected into HEK293T cells was as the control group. Cells were digested and plated into a 96-well microplate (Corning 3600) for 24 h following adding the substrate coelenterazine H into the medium at the final concentration of 5 uM. The agonist 8-OHDPAT or OB or both 8-OHDPAT and OB were added to the medium. The data were collected using the Tristar LB941 plate reader (Berthold Technologies, Bad Wildbad, Germany) and presented as "mBRET". The data were collected at every 5 mins in duration of 20 mins.

Cell transfection

HEK293T cells were cultured in the Dulbecco's modified Eagle's medium (DMEM, Invitrogen) medium containing 10% fetal bovine serum (FBS) and 0.1% $NaHCO_3$ (Sigma-Aldrich) in humidified atmosphere containing 5% CO_2 at 37□. For BRET assay, 1 μg plasmid was using for each well of 24-well plate. For western blotting experiment, 4ug plasmids was using for each well of 6-well plate. The plasmids were

introduced into the HEK293T cells according to the protocol of Lipofectamine 2000 reagent.

Statistical analysis

The data were analyzed using GraphPad Prism v5.0. All the data were presented as means ± SEM. The treatment group was compared with the control group by student's t-test or one-way ANOVA followed by a *post hoc* test including Sidak's multiple, Student-Newman-Keul's test or Dunnet test comparisons test. Differences were considered to be significant when the P value less than 0.05. All the experiments were repeated three times at least.

Conclusions

Taken together, we found that 5-HT1AR and OX2R could form heterodimers *in vitro* and *in vivo* and further affect the expression of the downstream signaling molecular including cAMP, calcium, p-ERK and p-CREB, which will not only promote our understanding of the role of 5-HT1AR and OX2R in the physiological processes but also provide new molecular mechanisms underlying the neurological diseases.

Author's contribution

Q.-Q.W, B.B and J.C conceived and designed the experiments; Q.-Q.W conducted the experiments and wrote the manuscript; C.-M.W and B.-H.C performed the data analysis; C.-Q.Y contributed to the cell culture; B.B and J.C supervised the project and wrote the manuscript.

Competing interests

The authors declare no conflicts of interest.

References

1.   Sexton, P.M. and A. Christopoulos, *To Bind or Not to Bind: Unravelling GPCR Polypharmacology.* Cell, 2018. **172**(4): p. 636-638.

2.   Erlandson, S.C., C. McMahon, and A.C. Kruse, *Structural Basis for G Protein-Coupled Receptor Signaling.* Annu Rev Biophys, 2018.

3.   Wei, L., et al., *Rosiglitazone Inhibits Angiotensin II-Induced Proliferation of Glomerular Mesangial Cells via the Galphaq/Plcbeta4/TRPC Signaling Pathway.* Cell Physiol Biochem, 2017. **44**(6): p. 2228-2242.

票旲籥Shao, W., et al., *Suppression of neuroinflammation by astrocytic dopamine D2 receptors via alphaB-crystallin.* Nature, 2013. **494**(7435): p. 90-4.

5.   Drevets, W.C., et al., *Serotonin-1A receptor imaging in recurrent depression: replication and literature review.* Nucl Med Biol, 2007. **34**(7): p. 865-77.

6.   Su, P., et al., *A dopamine D2 receptor-DISC1 protein complex may contribute to antipsychotic-like effects.* Neuron, 2014. **84**(6): p. 1302-16.

7.   Tena-Campos, M., et al., *Zinc Is Involved in Depression by Modulating G Protein-Coupled Receptor Heterodimerization.* Mol Neurobiol, 2016. **53**(3): p. 2003-2015.

8.   Fuxe, K., et al., *On the existence and function of galanin receptor heteromers in the central nervous system.* Front Endocrinol (Lausanne), 2012. **3**: p. 127.

9.   Lee, J.Y., et al., *Crystal structure of the human sterol transporter ABCG5/ABCG8.* Nature, 2016. **533**(7604): p. 561-4.

10.   Lukasiewicz, S., et al., *Dopamine D2 and serotonin 5-HT1A receptor interaction in the context of the effects of antipsychotics - in vitro studies.* J Neurochem, 2016. **137**(4): p. 549-60.

11.   Peng, Y., et al., *5-HT2C Receptor Structures Reveal the Structural Basis of GPCR Polypharmacology.* Cell, 2018. **172**(4): p. 719-730 e14.

12.   Basak, S., et al., *Cryo-EM structure of 5-HT3A receptor in its resting conformation.* Nat Commun, 2018. **9**(1): p. 514.

13.   Lian, P., et al., *Higher-Affinity Agonists of 5-HT1AR Discovered through Tuning the Binding-Site Flexibility.* J Chem Inf Model, 2015. **55**(8): p. 1616-27.

14.   Garcia-Garcia, A.L., et al., *Serotonin Signaling through Prefrontal Cortex 5-HT1A Receptors during Adolescence Can Determine Baseline Mood-Related Behaviors.* Cell Rep, 2017. **18**(5): p. 1144-1156.

15.   Rojas, P.S. and J.L. Fiedler, *What Do We Really Know About 5-HT1A Receptor Signaling in Neuronal Cells?* Front Cell Neurosci, 2016. **10**: p. 272.

16.   Borroto-Escuela, D.O., et al., *Fibroblast growth factor receptor 1- 5-hydroxytryptamine 1A heteroreceptor complexes and their enhancement of hippocampal plasticity.* Biol Psychiatry, 2012. **71**(1): p. 84-91.

17.   Terao, A., et al., *Age-related decline in hypocretin (orexin) receptor 2 messenger RNA*

levels in the mouse brain. Neurosci Lett, 2002. **332**(3): p. 190-4.

18. Wang, C., et al., *C-terminus of OX2R significantly affects downstream signaling pathways.* Mol Med Rep, 2017. **16**(1): p. 159-166.

19. Tang, J., et al., *The signalling profile of recombinant human orexin-2 receptor.* Cell Signal, 2008. **20**(9): p. 1651-61.

20. Guo, Y. and P. Feng, *OX2R activation induces PKC-mediated ERK and CREB phosphorylation.* Exp Cell Res, 2012. **318**(16): p. 2004-13.

21. Yelin-Bekerman, L., et al., *Hypocretin neuron-specific transcriptome profiling identifies the sleep modulator Kcnh4a.* Elife, 2015. **4**: p. e08638.

22. Korim, W.S., I.J. Llewellyn-Smith, and A.J. Verberne, *Activation of Medulla-Projecting Periformical Neurons Modulates the Adrenal Sympathetic Response to Hypoglycemia: Involvement of Orexin Type 2 (OX2-R) Receptors.* Endocrinology, 2016. **157**(2): p. 810-9.

23. Weller, C.M., et al., *Cluster headache and the hypocretin receptor 2 reconsidered: a genetic association study and meta-analysis.* Cephalalgia, 2015. **35**(9): p. 741-7.

24. Yin, J., et al., *Crystal structure of the human OX2 orexin receptor bound to the insomnia drug suvorexant.* Nature, 2015. **519**(7542): p. 247-50.

25. Scott, M.M., et al., *Hcrtr1 and 2 signaling differentially regulates depression-like behaviors.* Behav Brain Res, 2011. **222**(2): p. 289-94.

26. Harikumar, K.G., et al., *Bioluminescence Resonance Energy Transfer (BRET) Assay for Determination of Molecular Interactions in Living Cells.* Bio Protoc, 2017. **7**(22).

27. Pack, T.F., et al., *The dopamine D2 receptor can directly recruit and activate GRK2*

without G protein activation. J Biol Chem, 2018.

28.   Bon, N., et al., *Phosphate (Pi)-regulated heterodimerization of the high-affinity sodium-dependent Pi transporters PiT1/Slc20a1 and PiT2/Slc20a2 underlies extracellular Pi sensing independently of Pi uptake.* J Biol Chem, 2018. **293**(6): p. 2102-2114.

29.   Jambor, T., et al., *Parallel effect of 4-octylphenol and cyclic adenosine monophosphate (cAMP) alters steroidogenesis, cell viability and ROS production in mice Leydig cells.* Chemosphere, 2018.

30.   Gu, J., et al., *Maresin 1 attenuates mitochondrial dysfunction through the ALX/cAMP/ROS pathway in the cecal ligation and puncture mouse model and sepsis patients.* Lab Invest, 2018.

31.   Veremeyko, T., et al., *Cyclic AMP Pathway Suppress Autoimmune Neuroinflammation by Inhibiting Functions of Encephalitogenic CD4 T Cells and Enhancing M2 Macrophage Polarization at the Site of Inflammation.* Front Immunol, 2018. **9**: p. 50.

32.   Louis, T., et al., *Cyclic AMP-dependent plasticity underlies rapid changes in odor coding associated with reward learning.* Proc Natl Acad Sci U S A, 2018. **115**(3): p. E448-E457.

33.   Araujo, L.B., et al., *Effects of mineral trioxide aggregate, BiodentineTM and calcium hydroxide on viability, proliferation, migration and differentiation of stem cells from human exfoliated deciduous teeth.* J Appl Oral Sci, 2018. **26**: p. e20160629.

34.   de Seabra Rodrigues Dias, I.R., et al., *The Calcium-Induced Regulation in the Molecular and Transcriptional Circuitry of Human Inflammatory Response and*

Autoimmunity. Front Pharmacol, 2017. **8**: p. 962.

35.   Liao, C., Y. Zheng, and Y. Guo, *MYB30 transcription factor regulates oxidative and heat stress responses through ANNEXIN-mediated cytosolic calcium signaling in Arabidopsis.* New Phytol, 2017. **216**(1): p. 163-177.

36.   Conceicao, E.P., et al., *Effect of Early Overfeeding on Palatable Food Preference and Brain Dopaminergic Reward System at Adulthood: Role of Calcium Supplementation.* J Neuroendocrinol, 2016. **28**(5).

37.   Bergantin, L.B. and A. Caricati-Neto, *Challenges for the pharmacological treatment of neurological and psychiatric disorders: Implications of the Ca(2+)/cAMP intracellular signalling interaction.* Eur J Pharmacol, 2016. **788**: p. 255-260.

38.   Bai, B., et al., *Heterodimerization of human apelin and bradykinin 1 receptors: novel signal transduction characteristics.* Cell Signal, 2014. **26**(7): p. 1549-59.

39.   Sun, Y., et al., *Signaling pathway of MAPK/ERK in cell proliferation, differentiation, migration, senescence and apoptosis.* J Recept Signal Transduct Res, 2015. **35**(6): p. 600-4.

40.   Luo, D., et al., *N-Propargyl Caffeamide (PACA) Ameliorates Dopaminergic Neuronal Loss and Motor Dysfunctions in MPTP Mouse Model of Parkinson's Disease and in MPP(+)-Induced Neurons via Promoting the Conversion of proNGF to NGF.* Mol Neurobiol, 2018. **55**(3): p. 2258-2267.

41.   Ko, Y.H., et al., *6,7,4'-Trihydroxyisoflavone, a major metabolite of daidzein, improves learning and memory via the cholinergic system and the p-CREB/BDNF signaling pathway in mice.* Eur J Pharmacol, 2018.

42. Wang, B., et al., *Methamphetamine modulates the production of interleukin-6 and tumor necrosis factor-alpha via the cAMP/PKA/CREB signaling pathway in lipopolysaccharide-activated microglia.* Int Immunopharmacol, 2018. **56**: p. 168-178.

43. Sharma, P., S. Sharma, and D. Singh, *Apigenin reverses behavioural impairments and cognitive decline in kindled mice via CREB-BDNF upregulation in the hippocampus.* Nutr Neurosci, 2018: p. 1-10.

44. Tsuchimine, S., N. Sugawara, and N. Yasui-Furukori, *Increased levels of CREB in major depressive patients with antidepressant treatment.* Psychiatry Res, 2018.

45. Cheng, Z., et al., *Luciferase Reporter Assay System for Deciphering GPCR Pathways.* Curr Chem Genomics, 2010. **4**: p. 84-91.

46. Abe, M., et al., *Homodimer formation by the ATP/UTP receptor P2Y2 via disulfide bridges.* J Biochem, 2018.

47. Ji, B., et al., *Novel signaling of dynorphin at kappa-opioid receptor/bradykinin B2 receptor heterodimers.* Cell Signal, 2017. **31**: p. 66-78.

48. Scarlett, K.A., et al., *Agonist-induced CXCR4 and CB2 Heterodimerization Inhibits Galpha13/RhoA-mediated Migration.* Mol Cancer Res, 2018.

49. Liu, H., et al., *Heterodimerization of the kappa opioid receptor and neurotensin receptor 1 contributes to a novel beta-arrestin-2-biased pathway.* Biochim Biophys Acta, 2016. **1863**(11): p. 2719-2738.

50. Zhang, Y., et al., *Sorafenib inhibited cell growth through the MEK/ERK signaling pathway in acute promyelocytic leukemia cells.* Oncol Lett, 2018. **15**(4): p. 5620-5626.

51. Sharma, K., et al., *MeCP2 overexpression inhibits proliferation, migration and invasion*

of C6 glioma by modulating ERK signaling and gene expression. Neurosci Lett, 2018. **674**: p. 42-48.

52.   Zhang, X., et al., *Diethylstilbestrol regulates mouse gubernaculum testis cell proliferation via PLC-Ca(2+) -CREB pathway.* Cell Biochem Funct, 2018. **36**(1): p. 13-17.

53.   Gao, J., et al., *Harmine suppresses the proliferation and migration of human ovarian cancer cells through inhibiting ERK/CREB pathway.* Oncol Rep, 2017. **38**(5): p. 2927-2934.

54.   Sen, T., et al., *Activation of PERK Elicits Memory Impairment through Inactivation of CREB and Downregulation of PSD95 After Traumatic Brain Injury.* J Neurosci, 2017. **37**(24): p. 5900-5911.

55.   Yu, L.N., et al., *EphrinB-EphB Signaling Induces Hyperalgesia through ERK5/CREB Pathway in Rats.* Pain Physician, 2017. **20**(4): p. E563-E574.

56.   Li, Z., et al., *Resveratrol protects CA1 neurons against focal cerebral ischemic reperfusion-induced damage via the ERK-CREB signaling pathway in rats.* Pharmacol Biochem Behav, 2016. **146-147**: p. 21-7.

57.   Zhang, L., et al., *Tyrosine phosphatase STEP61 negatively regulates amyloid beta-mediated ERK/CREB signaling pathways via alpha7 nicotinic acetylcholine receptors.* J Neurosci Res, 2013. **91**(12): p. 1581-90.

58.   Wang, H., et al., *Antinociceptive effects of oxymatrine from Sophora flavescens, through regulation of NR2B-containing NMDA receptor-ERK/CREB signaling in a mice model of neuropathic pain.* Phytomedicine, 2013. **20**(11): p. 1039-45.

59.   Carlezon, W.A., Jr., R.S. Duman, and E.J. Nestler, *The many faces of CREB.* Trends Neurosci, 2005. **28**(8): p. 436-45.

60.   Li, L., et al., *The effects of Chinese medicines on cAMP/PKA signaling in central nervous system dysfunction.* Brain Res Bull, 2017. **132**: p. 109-117.

61.   Ge, C.L., et al., *Tongqiao Huoxue Decoction ameliorates learning and memory defects in rats with vascular dementia by up-regulating the Ca(2+)-CaMKII-CREB pathway.* Chin J Nat Med, 2015. **13**(11): p. 823-830.

62.   Xiao, X., et al., *The cAMP responsive element-binding (CREB)-1 gene increases risk of major psychiatric disorders.* Mol Psychiatry, 2017.

63.   Gu, X., et al., *Photoactivation of ERK/CREB/VMAT2 pathway attenuates MPP(+)-induced neuronal injury in a cellular model of Parkinson's disease.* Cell Signal, 2017. **37**: p. 103-114.

64.   Wang, X.L., et al., *Treatment with Shuyu capsule increases 5-HT1AR level and activation of cAMP-PKA-CREB pathway in hippocampal neurons treated with serum from a rat model of depression.* Mol Med Rep, 2018. **17**(3): p. 3575-3582.

65.   Borroto-Escuela, D.O., et al., *Dynamic modulation of FGFR1-5-HT1A heteroreceptor complexes. Agonist treatment enhances participation of FGFR1 and 5-HT1A homodimers and recruitment of beta-arrestin2.* Biochem Biophys Res Commun, 2013. **441**(2): p. 387-92.

66.   Zhen, J., et al., *Deep Brain Magnetic Stimulation Promotes Neurogenesis and Restores Cholinergic Activity in a Transgenic Mouse Model of Alzheimer's Disease.* Front Neural Circuits, 2017. **11**: p. 48.

67.   Rojas, P.S., et al., *Dual effect of serotonin on the dendritic growth of cultured hippocampal neurons: Involvement of 5-HT1A and 5-HT7 receptors.* Mol Cell Neurosci, 2017. **85**: p. 148-161.

68.   Noto, B., et al., *Increased adult neurogenesis in mice with a permanent overexpression of the postsynaptic 5-HT1A receptor.* Neurosci Lett, 2016. **633**: p. 246-251.

69.   Dupre, K.B., et al., *Effects of 5-HT1A receptor stimulation on D1 receptor agonist-induced striatonigral activity and dyskinesia in hemiparkinsonian rats.* ACS Chem Neurosci, 2013. **4**(5): p. 747-60.

70.   Meadows, S.M., et al., *Characterizing the differential roles of striatal 5-HT1A auto- and hetero-receptors in the reduction of l-DOPA-induced dyskinesia.* Exp Neurol, 2017. **292**: p. 168-178.

71.   Dupre, K.B., et al., *Striatal 5-HT1A receptor stimulation reduces D1 receptor-induced dyskinesia and improves movement in the hemiparkinsonian rat.* Neuropharmacology, 2008. **55**(8): p. 1321-8.

72.   Zheng, G., et al., *Revealing vilazodone's binding mechanism underlying its partial agonism to the 5-HT1A receptor in the treatment of major depressive disorder.* Phys Chem Chem Phys, 2017. **19**(42): p. 28885-28896.

73.   Riad, M., et al., *Chronic fluoxetine rescues changes in plasma membrane density of 5-HT1A autoreceptors and serotonin transporters in the olfactory bulbectomy rodent model of depression.* Neuroscience, 2017. **356**: p. 78-88.

74.   Le, J.J., et al., *Electroacupuncture regulate hypothalamic-pituitary-adrenal axis and*

enhance hippocampal serotonin system in a rat model of depression. Neurosci Lett, 2016. **615**: p. 66-71.

75.   Wang, Q., et al., *Elevated Hapln2 Expression Contributes to Protein Aggregation and Neurodegeneration in an Animal Model of Parkinson's Disease.* Front Aging Neurosci, 2016. **8**: p. 197.

76.   Barak, L.S., et al., *Pharmacological characterization of membrane-expressed human trace amine-associated receptor 1 (TAAR1) by a bioluminescence resonance energy transfer cAMP biosensor.* Mol Pharmacol, 2008. **74**(3): p. 585-594.